J. Biochem. 2011;149(1):91–101 doi:10.1093/jb/mvq122

JB THE JOURNAL OF BIOCHEMISTRY

Characterization of a novel rice kinesin O12 with a calponin homology domain

Received July 10, 2010; accepted October 6, 2010; published online November 3, 2010

Nozomi Umezu[1], Nobuhisa Umeki[2], Toshiaki Mitsui[2], Kazunori Kondo[1] and Shinsaku Maruta[1,*]

[1]Division of Bioengineering, Graduate School of Engineering, Soka University, Hachioji, Tokyo 192-8577 and [2]Laboratories of Plant and Microbial Genome Control, Graduate School of Science and Technology, Niigata University, Niigata 950-2181, Japan

*Prof. Shinsaku Maruta, Division of Bioinformatics, Graduate School of Engineering, Soka University 1-236 Tangi-machi, Hachioji, Tokyo 192-8577, Japan. Tel: +81 426 91 9443, Fax: +81 426 91 9312, e-mail: maruta@soka.ac.jp

Genomic analysis predicted that the rice (*Oryza sativa* var. *japonica*) genome encodes at least 41 kinesin-like proteins including the novel kinesin O12, which is classified as a kinesin-14 family member. O12 has a calponin homology (CH) domain that is known as an actin-binding domain. In this study, we expressed the functional domains of O12 in *Escherichia coli* and determined its enzymatic characteristics compared with other kinesins. The microtubule-dependent ATPase activity of recombinant O12 containing the motor and CH domains was significantly reduced in the presence of actin. Interestingly, microtubule-dependent ATPase activity of the motor domain was also affected by actin in the absence of the CH domain. Our findings suggest that the motor activity of the rice plant-specific kinesin O12 may be regulated by actin.

Keywords: actin/kinesin/plant/regulation/rice.

Abbreviations: CH, calponin homology; Co-NTA, cobalt nitrilotriacetic acid; GFP(S65T), green fluorescence protein mutated at S65T; IPTG, isopropyl-β-D-thiogalactopyranoside; KCH, calponin homology domain-containing kinesin; KHC, conventional kinesin heavy chain; KIF, kinesin superfamily protein; MD, motor domain; MES, 2-(N-morpholino)ethanesulphonic acid; MOPS, 3-(*N*-morpholino)propanesulphonic acid; MT, microtubule; NBD-ATP, 2′(3′)-O-[6-(*N*-(7-nitrobenz-2-oxa-1,3-diazol-4-yl)amino)hexanoic]-ATP; PIPES, 1,4-piperazinediethanesulphonic acid; PMSF, phenylmethylsulphonyl fluoride; TCA, trichloro acetic acid.

Kinesins constitute a superfamily of ATP-driven microtubule motor proteins that move along microtubules. Kinesins are essential to animal cells, and are known to be involved in diverse cellular functions such as transport of organelles and vesicles, spindle formation and elongation, chromosome segregation during cell division, microtubule dynamics and morphogenesis (*1–4*). Kinesin superfamily proteins (KIFs) have been well studied in animals, especially those from mice and humans. In contrast, only a few kinesins have been characterized in plants, mostly in *Arabidopsis thaliana* (*5–15*). The complete sequencing of the *Arabidopsis* genome led to the identification of 61 kinesin-like genes, the largest number of kinesins identified in a completely sequenced eukaryotic genome (*7*). Phylogenetic analysis of *Arabidopsis* kinesin motor domain (MD) sequences with other MD sequences revealed that some do not belong to any known family, and that some subfamilies are unique to *Arabidopsis* and perhaps to plants (*16*, *17*). These plant-specific kinesins may participate in specific plant functions including the formation of phragmoplasts evident at cell division, morphogenesis of the leaf trichome and flower morphogenesis (*5*, *6*, *18*, *19*).

In 2002, the entire genome of rice (*Oryza sativa*) was mapped, allowing genetic analyses related to plant function to be conducted. Within the rice genome, 41 genes that encode kinesin proteins have been reported (*20*). Previously, we succeeded in expressing the rice plant-specific kinesins and characterized their biochemical properties. K16, one of those novel rice plant-specific kinesins, showed several unique enzymatic characteristics compared with conventional kinesin (*21*). Its most interesting property is that the ADP-free K16 motor domain (K16MD) is very stable, in contrast to conventional kinesin, which is very labile in an ADP-free state (*22*). Recently, we determined the crystal structure of the K16MD in complex with MgADP (*23*). The overall structure of the K16MD is similar to that of conventional kinesin MDs. However, the neck linker of the ADP-bound K16MD showed an ordered conformation in a position quite different from that observed in conventional kinesin. This conformation may reflect the unique enzymatic characteristics of rice kinesin K16, which, in turn, may be related to plant-specific physiological roles.

In the present study, we focused on another novel rice plant kinesin, O12, found in the rice genome. Kinesin O12 has its MD in the C-terminal and belongs to the kinesin-14 subfamily (Figs 1 and 2). O12 is unique in that it contains a calponin homology (CH) domain at its N terminus. Calponin is an actin-binding protein, and it is believed to regulate actin-activated myosin ATPase activity (*24*). As the CH domains of kinesins are homologous to calponin, the CH domain of kinesin O12 is also believed to bind to the actin cytoskeleton. Recently, CH domain-containing kinesins (KCHs) have been reported in cotton (*Goossypium hirsutum*) and *Arabidopsis* (*8*, *25–29*). To date, KCHs have been reported only in plants; none have been found in animals. The cytoskeleton, especially microtubules and actin, is necessary to maintain the shape of plant cells. During cellular division, actin also has supplemental functions in the regulation of microtubules (*30–32*). Therefore, plant kinesins that can interact with actin may play major physiological roles in plant cells. However, little is known about the biochemical enzymatic characteristics of KCHs. We have characterized higher plant kinesin O12 in terms of its biochemical analysis, and the effect of the CH domain and actin on kinesin ATPase activity. The results indicate that the function of plant kinesins containing a CH domain may be regulated by actin.

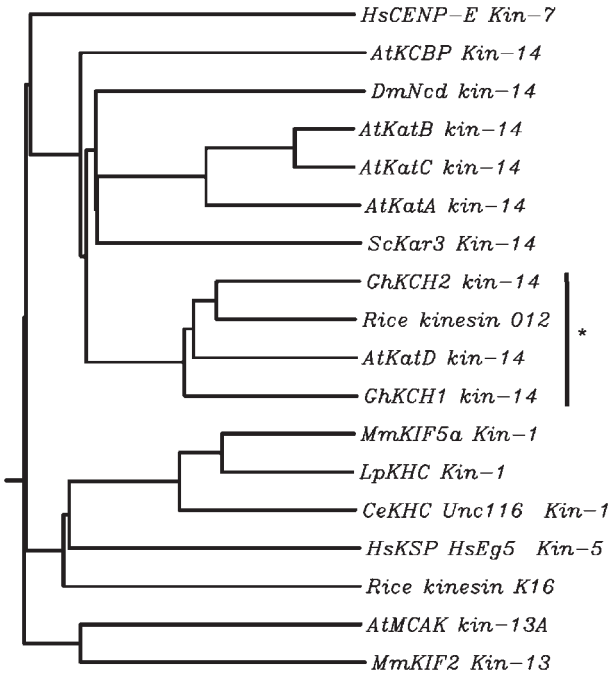

Fig. 1 Phylogenetic tree of kinesins. Phylogenetic analysis of the rice kinesin O12 and other plant kinesins, as well as representative animal kinesins. Phylogenetic analysis was carried out using the amino acid sequences of kinesins. The phylogenetic analysis was performed with online software ClustalW version 1.81 (provided by Kyoto University Bioinformatics Center, http://align.genome.jp/). A vertical line indicates the kinesins with CH domains. An asterisk indicates the rice kinesin O12.

Materials and Methods

Bioinformatics of rice kinesins

Phylogenetic analysis was carried out using the amino acid sequences of kinesins. The amino acid sequences of kinesins can be found in KOME (Knowledge-based Oryza Molecular Biological Encyclopedia, http://cdna01.dna.affrc.go.jp/cDNA/) and the Kinesin Home Page (http://www.cellbio.duke.edu/kinesin/). The accession numbers of kinesins used in the analysis are: CeKHC (Unc116) L19120, DmNcd X52814, HsKSP (HsEg5) U37426, HsCENP-E, Z15005, LpKHC J05258, MmKIF2, D12644 MmKIF5a AF067179, ScKar3 M31719, AtKatA D11371, AtKatB D21137, AtKatC D21138, AtKatD AF080249, AtKCBP L40358, AtMCAK NM 180267, GhKCH1 AY695833, GhKCH2 EF432568, rice kinesin K16 AK068672 and rice kinesin O12 AK065586. The phylogenetic analysis was performed by using ClustalW, version 1.81, provided online by the Kyoto University Bioinformatics Center (http://align.genome.jp/). Prediction of coiled coils in O12 was performed by using the COILS program online (http://www.ch.embnet.org/software/COILS_form.html).

Cloning of kinesin O12 and its motor domain

The O12 plasmid (accession number: AK065586, clone name: J013034O12) was supplied by the National Institute of Agrobiological Science (NIAS). The DNA fragment encoding the C-terminal motor domain (amino acids 372–717), O12MD, was amplified by PCR using the LamdaFLC-J013034O12 plasmid. The set of forward and reverse primers was 5′-AAGGATCCGAAAGGA AATATTAGAGTATACTGTCGAGTG-3′ and 5′-AAGGATCCT TAGTTTGCTTTTGCTGCACCAAGCTCAACTGA-3′ containing a BamHI site. The gel-purified PCR fragment was cloned into the BamHI site of the pET15b vector (Merk, Darmstadt, Germany). The cDNA sequence was confirmed using a SQ-5500 sequencer (Hitachi, Tokyo, Japan). The DNA encoding O12CH-MD, the fragment from the CH domain to the MD (amino acids 25–717), was amplified by PCR using the LamdaFLC-J013034O12 plasmid. The set of forward and reverse primers was 5′-AAACTCGAGAGACGG TATGATGCGGCAAGTTGG-3′ and 5′-AAGGATCCTTATTTG AGCTCTCTAACCTCACTGCC-3′ containing XhoI and BamHI sites. The gel-purified PCR product was digested with XhoI/BamHI and ligated into pColdI vector (Takara, Shiga, Japan).

Transformation and purification of Escherichia coli expressing recombinant O12

The constructed plasmids were transformed into *E. coli* BL21 (DE3) (Invitrogen, CA, USA) for large-scale expression of the recombinant kinesin proteins. Transformations were selected on L-plates with 100 mg/ml ampicillin. *Escherichia coli* was cultured for 3 h at 37°C and 180 rpm in 61 L-broth containing 100 mg/ml ampicillin. Expression of O12MD was induced at absorbance value at 600 nm of 0.6–0.7, and 0.1 mM IPTG and 0.1 mM DTT were added. Incubation was then continued for 4 h at 37°C. Expression of O12CH-MD was induced by shock on ice at absorbance value at 600 nm of ~0.5, 0.2 mM IPTG and 0.1 mM DTT were added. Incubation was then continued for 24 h at 15°C. The cells were harvested by centrifugation at 5000 *g* for 15 min using a no. 30 rotor (Hitachi Himac CR22G), suspended in HEM buffer (10 mM HEPES pH 7.2, 1 mM $MgCl_2$, 1 mM EGTA, 25 mM NaCl and 1 mM DTT) and stored at −80°C.

Purification of rice kinesins O12MD and O12CH-MD

The frozen cells were thawed, suspended in 20 ml sonication buffer (20 mM MOPS pH 7.0, 300 mM NaCl, 1 mM $MgCl_2$, 0.1 mM ATP, 0.2 mM β-mercaptoethanol, 0.5 mM PMSF, 2 mg/ml leupeptin, 1 mg/ml aprotinin and 1 mg/ml pepstatin A) and then subjected to five cycles of 30-s sonication and 1 min on ice with an Ultra S homogenizer (VP-30S, Taitec, Saitama, Japan) at micro tip limit 5 and a duty cycle of 50%. Samples were then centrifuged at 200,000 *g* for 1 h using a 70 Ti rotor (Beckman Coulter, CA, USA Optima XL-90 ultracentrifuge). The supernatant was applied to a Co-NTA column (Talon® Metal Affinity Resin, Takara), which had been equilibrated with equilibrium buffer (20 mM MOPS pH 7.0, 300 mM NaCl, 1 mM $MgCl_2$, 0.1 mM ATP and 0.2 mM β-mercaptoethanol). The column was then washed with 300 ml wash buffer (10 mM imidazole-HCl pH 7.0 in equilibrium buffer) and protein was eluted with elution buffer (150 mM imidazole-HCl

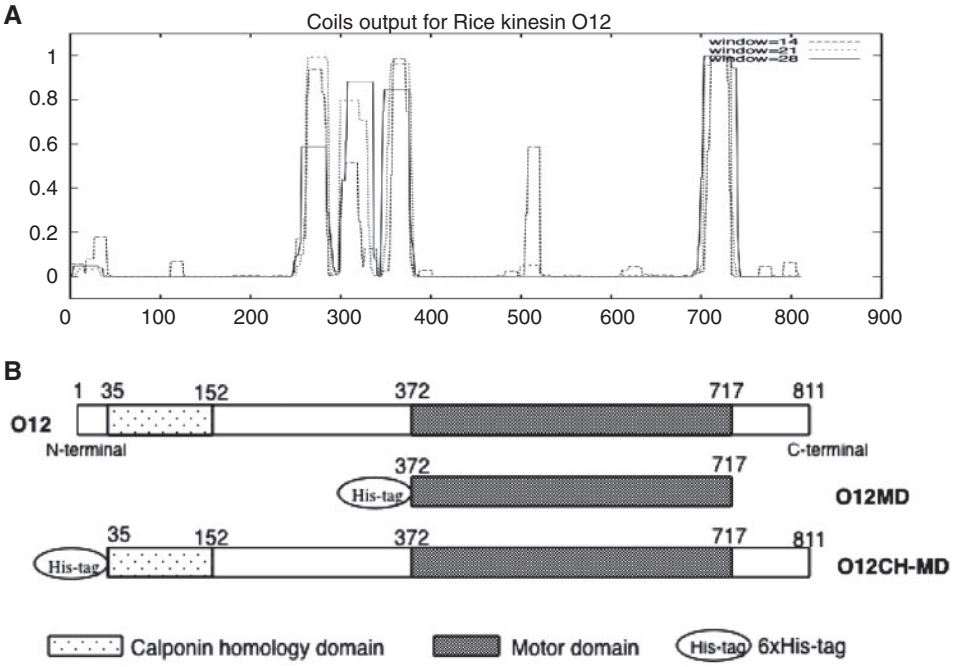

Fig. 2 Sequence analysis of O12. (A) Coiled-coil regions of O12. The coiled coils of O12 were determined by COILS version 2.2 (provided by EMBnet http://www.ch.embnet.org/software/COILS_form.html). The horizontal axis represents the position of the amino acid residues, and the vertical axis represents the probability of the formation of a coiled-coil. The coiled-coils appeared in the center (about 245–380 amino acids) and C-terminal (about 700–730 amino acids). (B) Schematic of O12 structure. The motor domain is gray, and the CH domain is shown in dots. Numbers refer to the corresponding amino acids. O12 has a CH domain at the N terminal, and motor domain at the C terminal. O12MD consisted of amino acids 372–717 (37.8 KDa), and O12CH-MD consisted of amino acids 35–717 (74.5 KDa). A His-tag was added to the N terminal of each recombinant kinesin.

pH 7.0 in equilibrium buffer). The elution buffer containing the protein was collected in fractions. Purity was assessed by SDS–PAGE. Purified kinesin was concentrated by centrifugation at 5000 *g* at 4°C using a Vivaspin 20 (100,000 MWCO PES, Sartorius Stedim, Goettingen, Germany). Kinesin was then dialysed with buffer (300 mM NaCl, 75 mM Tris–HCl pH 7.5, 0.2 mM ATP, 0.2 mM $MgCl_2$ and 0.5 mM DTT) and stored at −80°C until use.

Purification and polymerization of tubulin

Tubulin was purified from porcine brain as described by Hackney (*33*). To polymerize the tubulin in buffer (100 mM Pipes pH 6.8, 1 mM EGTA, 1 mM $MgCl_2$ and 1 mM GTP), it was incubated for 30 min at 37°C, and then taxol was added to a final concentration of 10 μM. The taxol-stabilized microtubules (MTs) were pelleted by centrifugation at 80,000 rpm for 15 min at 37°C (Hitachi Himac CS 120GX), the supernatant was aspirated off, and the MT pellet was homogenized in buffer (100 mM Pipes pH 6.8, 1 mM EGTA, 1 mM $MgCl_2$, 1 mM GTP and 10 μM taxol).

Purification of actin

Actin was purified from chicken skeletal muscle according to the method reported by Mommaerts (*34*). The chicken skeletal muscle was minced twice and washed in a buffer containing 0.15 M KPi pH 6.5, 0.3 M KCl, 2 mM ATP, 1 mM $MgCl_2$. The sample was left on ice for 15 min and then centrifuged at 8,000 rpm for 10 min at 4°C (Hitachi Himac CR22G). The precipitate was washed with cold water and filtered using cheesecloth, which was repeated three times. The sample was then washed twice with 0.4 % $NaHCO_3$ and very quickly washed twice with cold water. Finally, the sample was washed five times with cold acetone at −20°C, dried on filter paper and stored at −30°C.

The acetone powder was immersed in G buffer (0.2 mM ATP, 0.2 mM $CaCl_2$, 0.5 mM DTT, adjust pH 8–8.3 by Tris-base) for 20 min at 0°C. The sample was filtered using a Buechner funnel. The filtrate was centrifuged at 35,000 rpm for 30 min at 4°C and supernatant was then filtered with Whatman 541 filter paper. $MgCl_2$ (1 mM) and 0.1 M KCl were added to the filtrate and stirred by hand. This sample was incubated at 25°C for 15 min, then on ice for 1 h. Additional KCl was added to final concentration 0.6 M and incubated for 30 min on ice. The sample was centrifuged 35,000 rpm for 3 h at 4°C. The precipitate was rinsed twice with cold water and homogenized with G buffer, followed by dialysis in G buffer for 48 h, with buffer changed every 12 h. Then, G-actin was polymerized to F-actin by addition of $MgCl_2$/KCl. F-actin was stored on ice.

ATPase assay

O12MD and conventional kinesin MD (KIF5A MD) (1 μM each) were filtered through a Sephadex G-50 fine column to remove ATP and pre-incubated at 25°C for 5 min in 25 mM NaCl, 30 mM Tris–HCl pH 7.5, 3 mM $MgCl_2$, 0.1 mM EDTA, 1 mM EGTA, 1 mM β-mercaptoethanol and in the absence or presence of 5 μM MT. Adding 1 mM ATP started the ATPase reaction. The ATPase activity of kinesins was stopped by the addition of 10% TCA. The released Pi was measured by the method of Youngburg and Youngburg (*21*, *35*, *36*).

Fluorescence stopped-flow measurements

Fluorescence stopped-flow measurements were carried out with an SX-20 stopped flow apparatus (Applied Photo Physics). ATP binding and ADP release were monitored by fluorescence change of the fluorescent ATP analogues, NBD-ATP and NBD-ADP, with an excitation wavelength of 475 nm at 25°C. For emission, a cut-off filter of 495 nm was used as described in our previous report (*21*). The nucleotide to protein ratio was kept at 5. The buffer conditions were as follows: 20 mM Pipes pH 6.8, 3 mM $MgCl_2$, 0.1 mM EDTA and 0.1 mM EGTA. NBD-ATP was synthesized according to Maruta *et al.* (*37*).

ATPase assay with F-actin

ATPase assays were carried out at 25°C in 25 mM NaCl, 30 mM Tris–HCl pH 7.5, 3 mM $MgCl_2$, 0.1 mM EDTA, 1 mM EGTA, 1 mM β-mercaptoethanol and 1 μM O12MD, 1 μM 012CH-MD, or 0.1 μM KIF5A MD, in the presence or absence of 5 μM MT, and 0-20 μM F-actin. The ATPase reaction was started by adding 1 mM ATP.

Actin cosedimentation assays

The kinesins were centrifuged at 80,000 rpm for 10 min at 4°C (Hitachi Himac CS 120). Protein concentrations were then determined by the Bradford assay. The kinesin (2 μM) and F-actin (1–25 μM) were then centrifuged at 80,000 rpm for 10 min at 4°C (Hitachi Himac CS 120). Equal amounts of the resultant pellets and supernatants were separated by SDS–PAGE gradient gel (7.5–20%). The data were analyzed by an image analyser (Image Gauge V4.23).

Localization of O12 tail fused with GFP in onion cell

The DNA fragment encoding the N-terminal tail domain and coiled-coil region (1–1116 bp), O12-tail, was amplified by PCR using the LamdaFLC-J013034O12 plasmid. The set of forward and reverse primers was 5′-AAGGATCCATGATGGCCGCGGCGGT CGAGGAGGAGGAG-3′ and 5′-AAGGATCCACCACCTTTAA GGTCCTGTATTTGGTTGTATAATTTG-3′ containing a BamHI site. The gel-purified PCR fragment was cloned into the BamHI site of the p-GFP in a pUC18 vector (*38*). The O12-tail-GFP plasmid construct was used for expression in plant cells. Transgenic cell lines were established using onion cells. Onion epidermal cells were cultured on 0.6% Gelrite with 2,4-D-free MS medium at room temperature. The cells were bombarded with gold particles coated with O12-tail-GFP plasmid DNA by using a biolistic particle delivery system (Model PDS-1000/He, Bio-Rad, CA, USA). Twelve hours after bombardment, O12-tail-fused GFP was observed in onion cells using a confocal laser scanning microscope (upright microscope BX61, Olympus, Tokyo, Japan). Actin filament in the onion cell was also stained with rhodamine-phalloidin (Invitrogen) after fixing the cell with formaldehyde.

Results

Classification of novel rice kinesin O12

A phylogenetic tree was created with the online software ClustalW by inputting the amino acid sequences of some of the representative subfamilies of kinesins, including plant-specific kinesins and particularly the kinesins classified as kinesin-14 (Fig. 1). Using BLAST analysis, O12 was found to be a member of the kinesin-14 group, suggesting the presence of the CH domain. A phylogenetic tree was constructed using representative animal/plant kinesins that fall into the kinesin-14 family, along with other plant kinesins containing the CH domain (KCHs). The results indicated that O12 belongs to the kinesin-14 group. Within the kinesin-14 group, O12 was classified into the group of CH domain-containing proteins (Fig. 1 shown in bold). Because KCHs have not yet been observed in animals, they may have plant-specific functions.

To predict the coiled-coil region, we input the entire O12 amino acid sequence into COILS software, version 2.2 (Fig. 2A). The vertical axis shows probability and the horizontal axis shows the residue number. The diagram in Fig. 2B shows the total length and primary structure of O12, purified O12MD and O12CH-MD. Interestingly, coiled-coil regions were observed at both center (N terminal side of Motor doamin) and C terminal of O12MD. Other KCHs classified as members of the kinesin-14 family with CH domain also showed a similar distribution of coiled-coil regions. In contrast, the kinesin-14 family members without a CH domain contain a coiled-coil region only at the N terminal. Therefore, the coiled-coil region at the C terminal of KCH including O12 may have a specific physiological functional role.

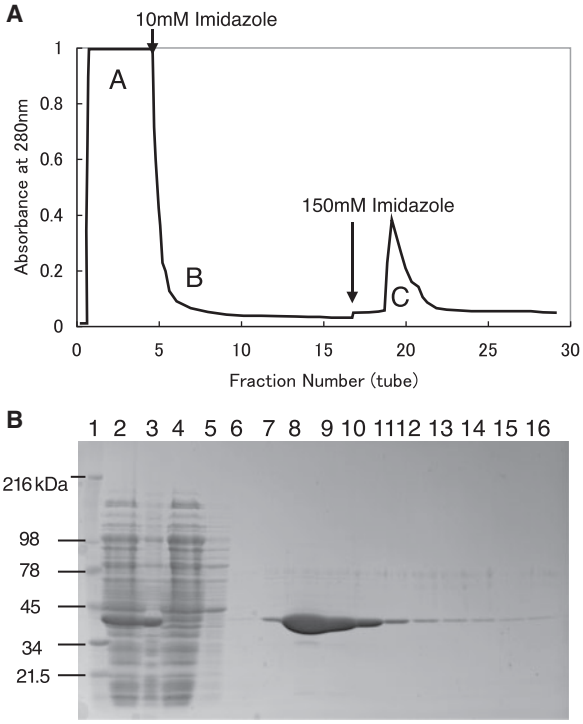

Fig. 3 Affinity purification of rice kinesin protein on Co-NTA. (A) An elution diagram showing the O12MD purified on Co-NTA. After loading of the sample, the column was washed for ~1.5 h at 2.7 ml/min with wash buffer (300 mM NaCl, 20 mM MOPS-NaOH pH 7.0, 1 mM $MgCl_2$, 0.1 mM ATP, 0.2 mM β-mercaptoethanol and 10 mM imidazole pH 7.0). The desired protein was eluted with 150 mM imidazole–HCl pH 7.5 in wash buffer. (B) Purity was assessed by SDS 7.5–20% gradient gel electrophoresis, which gave a single band on Coomassie-stained gels. Lane 1, a molecular weight marker (216 kDa myosin, 98 kDa phospholyase b, 78 kDa BSA, 45 kDa ovalbumin, 34 kDa carbonic anhydrase, and 21.5 kDa trypsin inhibitor); Lane 2, supernatant after the centrifugation; Lane 3, ppt is the precipitate of lysate; Lane 4, peakA is one fraction corresponding to the first peak in A at Fig. 3A; Lane 5, wash B is one fraction of eluted wash buffer and Lanes 6–16, peak C is whole fractions corresponding to the peak C at Fig. 3A.

Preparation of rice kinesin O12

The O12 motor domain (O12MD) (372–717 amino acids) and the region between the CH domain and the motor domain (O12CH-MD) (35–717 amino acids) was expressed in *E. coli* and purified as described in 'Materials and Methods' section. Figure 3A shows the elution pattern of O12MD fused with His-tag from the Co-NTA column. O12MD was eluted from the column at 150 mM imidazole. The purity of the O12MD (37.8 kDa) was confirmed by SDS–PAGE. As shown in Fig. 3B, highly purified O12MD was obtained. O12CH-MD (74.5 kDa) was also purified with the same methods at the high purity almost similar to that of O12MD. We have also expressed the O12 CH domain to examine the interaction with actin. However, the O12 CH domain expressed by *E. coli* was insoluble in the physiological buffer. Therefore, the insoluble O12 CH domain was not used for the further study.

ATPase activity

The basal and microtubule-activated ATPase activity of the rice kinesin MD was measured at 25°C in the

Table I. ATPase activity of O12MD and a conventional kinesin. K_{MT} indicates the microtubule concentration at Vmax/2.

	Hydrolysis (Pi mol/kinesin mol/min)		
	−MTs	+MTs	K_{MT} (μM)
Rice kinesin O12	1.19	90.6	3.7
Conventional kinesin	2.86	2810	0.65

MT, microtubule.

buffer of 25 mM NaCl, 30 mM Tris–HCl pH 7.5, 3 mM $MgCl_2$, 0.1 mM EDTA, 1 mM EGTA, 1 mM β-mercaptoethanol and proteins. As shown in Table I, in the absence of MT, the basal steady-state ATPase activity of O12MD was much lower (1.19 P_i mol/site mol/min) than that of conventional mouse brain kinesin KIF5A (2.86 P_i mol/site mol/min). In the presence of MT, the ATPase activity of O12MD was enhanced by ~70-fold (Table I and Fig. 4A). On the other hand, the ATPase activity of KIF5A MD was enhanced by ~1,000-fold. We have previously demonstrated that, for other plant kinesins, the magnitude of ATPase activity enhancement by MT was also much lower than that for mouse brain kinesin (*21*). In contrast, MTs are known to significantly accelerate the ATPase activity of conventional kinesin. These results suggested that the interaction between plant kinesin O12MD and animal-derived MTs is weaker than that of conventional kinesin.

In observations of ionic strength dependency, O12MD activity decreased when the concentration of NaCl increased (Fig. 4B). In the absence of MT, no dependence on ionic strength was observed. This characteristic was similar to that of K16 (*21*). In terms of pH dependence, O12MD showed the highest activity at pH 6.5 (Fig. 4C). For conventional kinesin, we observed a maximum activity peak at pH 7.0 under the same experimental condition. In plant cells, the pH of the vacuole is approximately 5.5, and cellular cytoplasm has a pH range of 6.8–7.0. The slightly shifted pH of O12 may be related to its physiological roles in plant cells.

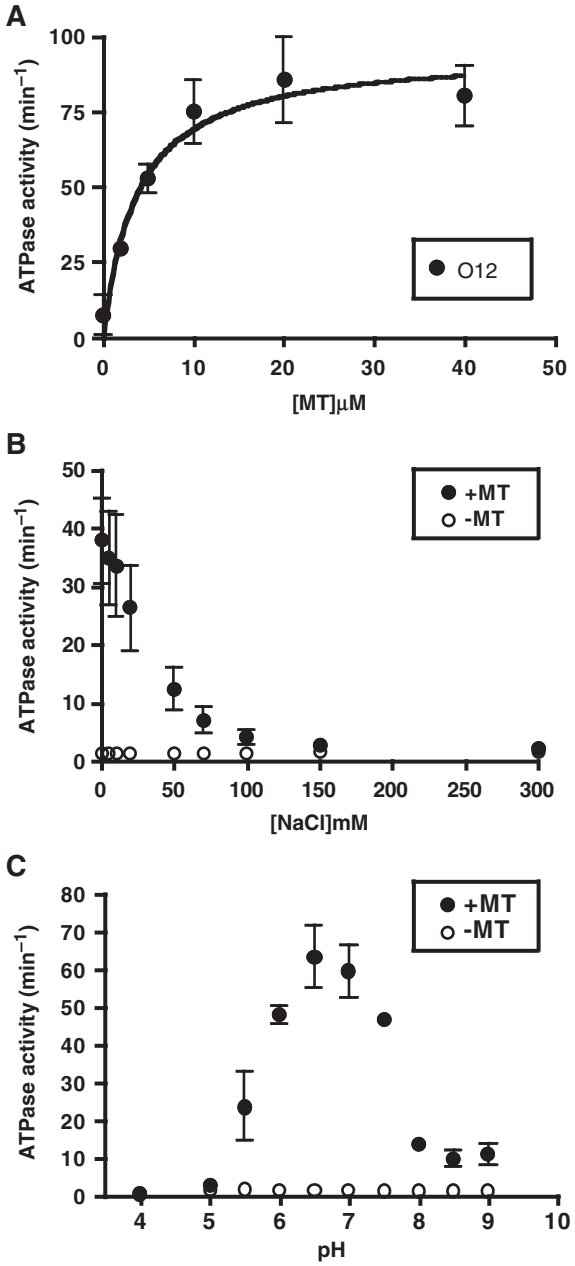

Fig. 4 ATPase assay of O12MD. (A) Microtubule (MT) concentration dependence of the ATPase activity of O12MD. ATPase assays were carried out at 25°C in 30 mM Tris–HCl pH 7.5, 3 mM $MgCl_2$, 0.1 mM EDTA, 1 mM EGTA, 1 mM β-mercaptoethanol, 1 μM O12MD and 0–40 μM microtubule. ATPase reactions were started by adding 1 mM ATP. The K_{MT} value was 4.82 μM. (B) NaCl concentration dependence of the ATPase activity of O12MD. ATPase assays were carried out as in (A) but with the addition of 0–300 mM NaCl in the absence (open circles) or presence (closed circles) of 5 μM microtubule. (C) pH dependence of the ATPase activity of O12 MD. ATPase assays were carried out as in (A), but in the absence (open circles) or presence (closed circles) of 5 μM microtubule and replacing 30 mM Tris–HCl pH 7.5 with the following buffers: for pH 4.0–5.0, acetate–NaOH; for pH 5.5–6.5, MES-NaOH; for pH 7.0–7.5, MOPS-NaOH and for pH 8.0–9.0, Tris–HCl.

Stopped-flow experiments on NBD-ATP binding to O12MD

The fluorescent ATP analogue NBD-ATP, which changes its fluorescent intensity during hydrolysis, was utilized for the kinetic studies of O12. The first phase of binding of NBD-ATP to O12MD under pseudo-first-order conditions with [NBD-ATP]> [O12MD] was examined by stopped-flow measurement. The nucleotide to protein ratio was kept at five as a compromise between achieving strictly first-order kinetics and maintaining a measurable fluorescence change relative to the background signal. NBD-ATP binding resulted in increasing NBD-ATP fluorescence intensity (Fig. 5A and C). The time course of the increase in NBD-ATP fluorescence was identical for successive pushes in the stopped-flow apparatus. The data were best fitted by an exponential curve. With low NBD-ATP concentrations (≤5 μM), the observed rates of the exponential phase increased linearly as a function of NBD-ATP concentration (Fig. 5B and D). The data gave the extremely low second-order rate constant of $3.94 \times 10^{-4}\,\mu M^{-1}\,s^{-1}$ in the absence of MT. In the presence of MT, the second-order rate constant was significantly accelerated to $1.50\,\mu M^{-1}\,s^{-1}$

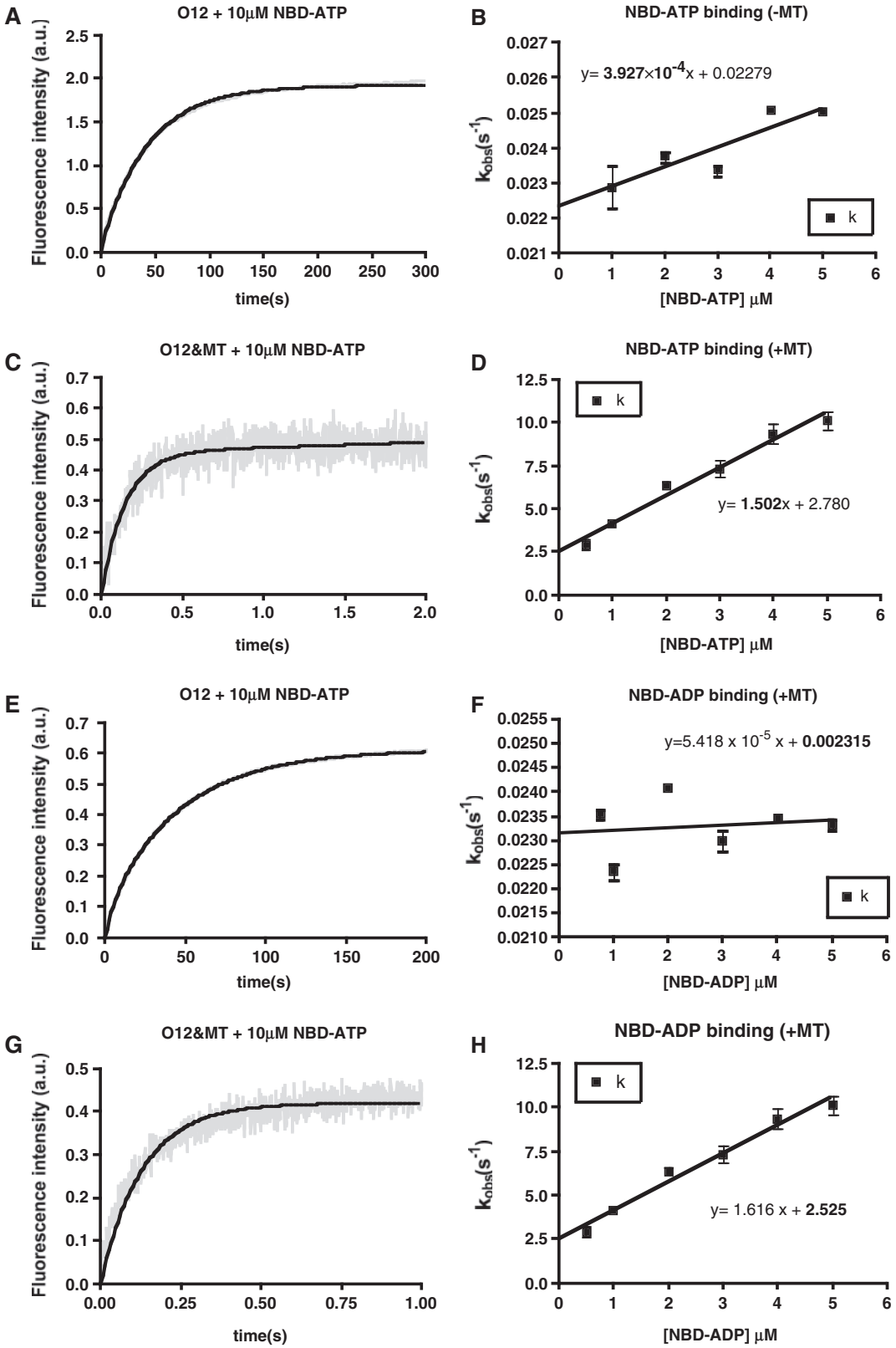

Fig. 5 Kinetic analysis of O12MD. (A) ATP binding in the absence of microtubule (MT). Fluorescence transients observed upon addition of excess NBD-ATP (final concentration, 10 μM) to O12MD (final concentration, 2 μM) in the stopped-flow apparatus. The buffer conditions were as follows: 20 mM Pipes-NaOH pH 6.8, 3 mM $MgCl_2$, 0.1 mM EDTA, 0.1 mM EGTA at 25°C. Time point zero indicates the time at which the flow stopped. The superimposed lines were least-mean-square fitted to the exponential curve. The reaction was monitored for NBD fluorescence intensity. (B) The observed exponential rate constant of the first transient phase was plotted as a function of NBD-ATP concentration from 1–5 μM NBD-ATP. For O12MD, the data provided the first-order rate constant of $3.94 \times 10^{-4}\,\mu M^{-1}\,s^{-1}$for NBD-ATP binding in the absence of MT during the initial fast phase. (C) ATP binding in the presence of MT. Fluorescence transients were observed upon addition of excess NBD-ATP (final concentration, 5 μM) to O12MD (final concentration, 1 μM) and MT (final concentration, 1.25 μM) in the stopped-flow apparatus. The buffer conditions were the same as in (A), but with the addition of MT and 10 μM taxol. The superimposed lines are

Table II. Experimentally determined rate constants for O12 and comparison with other kinesins.

	Conventional	Eg5	Ncd	K16	O12
ATP binding −MT ($\mu M^{-1}s^{-1}$)	5.88[a]	0.08[b]	0.005[c]	4.35[a]	3.94×10^{-4}
ATP binding +MT ($\mu M^{-1}s^{-1}$)	500[d]	3.4[e]	1.1[f]	N.D.	1.50
ADP release −MT (s^{-1})	0.02[d]	0.05[b]	0.0011[c]	N.D.	0.024
ADP release +MT (s^{-1})	300[d]	43.4[e]	3.9[f]	72	2.53

[a]Umeki *et al*., 2006 (*21*), [b]Cochran *et al*., 2006 (*40*), [c]Shimizu *et al*., 1995 (*35*), [d]Ma and Taylor 1997 (*39*), [e]Cochran *et al*., 2004 (*41*), [f]Mackey and Gilbert 2000 (*42*). MT, microtubule.

and reached the level of other kinesins with C-terminal motor domains. However, ATP initial binding step was relatively very slow for O12 compared with conventional kinesin (Table II).

Stopped-flow experiments on ADP binding and release by O12

Subsequently, we examined the kinetics of NBD-ADP binding to and release from O12. NBD-ADP binding was measured according to the methods of NBD-ATP binding. NBD-ADP concentration-dependent rates are plotted in Fig. 5F. The rates of NBD binding increased linearly as a function of NBD-ADP concentration. The slope of the plotted line gave the second-order rate constant of $5.48 \times 10^{-5}\,\mu M^{-1}\,s^{-1}$ for NBD-ADP binding to O12. The binding and release of NBD-ADP by O12 can be considered as single-step equilibrium reaction. The intercept of the vertical axis in Fig. 5F shows the apparent rate of release of NBD-ADP from O12. The rate of ADP release was $0.0024\,s^{-1}$ in the absence of MT. In the presence of MT, the rate of ADP release was accelerated to $2.53\,s^{-1}$ (Fig. 5H).

Interaction of O12 with actin

The CH domain is believed to interact with actin. However, the physiological function of the CH domain is still obscure. Moreover, biochemical studies on the interaction between KCH and actin have not yet been performed. We measured the ATPase activity of O12CH-MD in the presence of actin at 25°C in the buffer of 25 mM NaCl, 30 mM Tris–HCl pH 7.5, 3 mM $MgCl_2$, 0.1 mM EDTA, 1 mM EGTA, 1 mM β-mercaptoethanol and proteins. The ATPase activity of O12CH-MD was reduced by 20% in an actin concentration-dependent manner (Fig. 6A). The decrease in ATPase activity reached a plateau at 10 μM actin. From the data in Fig. 6A, the apparent inhibition

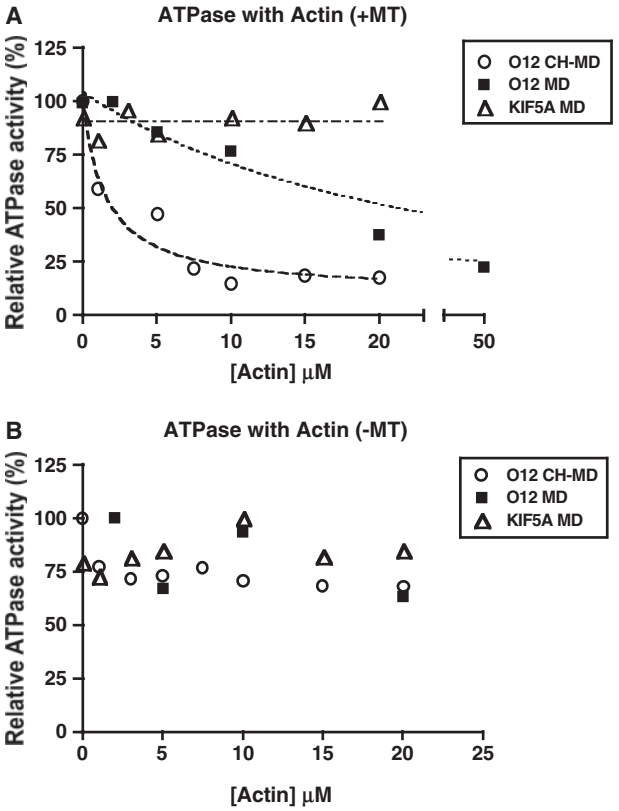

Fig. 6 Actin concentration dependence of the ATPase activities of kinesins. ATPase assays were carried out at 25°C in 25 mM NaCl, 30 mM Tris–HCl pH 7.5, 3 mM $MgCl_2$, 0.1 mM EDTA, 1 mM EGTA, 1 mM β-mercaptoethanol and 1 μM of each kinesin (O12CH-MD, O12MD and KIF5A MD), in the presence (A) or absence (B) of 5 μM microtubule (MT) and 0–20 (or 50) μM F-actin. The ATPase reaction was started by adding 1 mM ATP. O12CH-MD and O12MD demonstrated ATPase activity regulated by F-actin. The Ki of O12CH-MD and O12MD were ~2 μM and 20 μM, respectively. The conventional kinesin KIF5A MD was not regulated by actin, and no kinesins were regulated in the absence of microtubule.

least-mean-square fitted to the exponential curve. (D) The observed exponential rate constant of the first and rapid transient phases were plotted as a function of NBD-ATP concentration from 0.5–5 μM NBD-ATP. For O12MD, the data provided the second-order rate constant $1.50\,\mu M^{-1}s^{-1}$ for NBD-ATP binding in the presence of MT during the initial fast phase. (E) ADP binding in the absence of MT. Fluorescence transients observed upon addition of excess NBD-ADP (final concentration 5 μM) to O12MD (final concentration 1 μM) in the stopped-flow apparatus. The buffer conditions were the same as in (A). The superimposed lines are least-mean-square fitted to the exponential curve. (F) The observed exponential rate constants of the fluorescence were plotted as a function of NBD-ADP concentration from 0.5–5 μM NBD-ADP. The intercept of the vertical axis shows the apparent rate of release of NBD-ADP from O12. For O12MD, the data provided the second-order rate constant $0.0024\,s^{-1}$ for NBD-ADP release from O12 in absence of MT. (G) ADP binding in the presence of microtubule (MT). Fluorescence transients observed upon addition of excess NBD-ADP (final concentration 5 μM) to O12MD (final concentration 1 μM) and MT (final concentration 1.25 μM) in the stopped-flow apparatus. The buffer conditions were the same as in (C). The superimposed lines are least-mean-square fitted to the exponential curve. (H) The ADP release rate constant. The observed exponential rate constants of the fluorescence were plotted as a function of NBD-ADP concentration from 0.5–5 μM NBD-ADP. The intercept of the vertical axis shows the apparent rate of release of NBD-ADP from O12. For O12MD, the data provided the second-order rate constant $2.53\,s^{-1}$ for NBD-ADP release from O12 in the presence of MT.

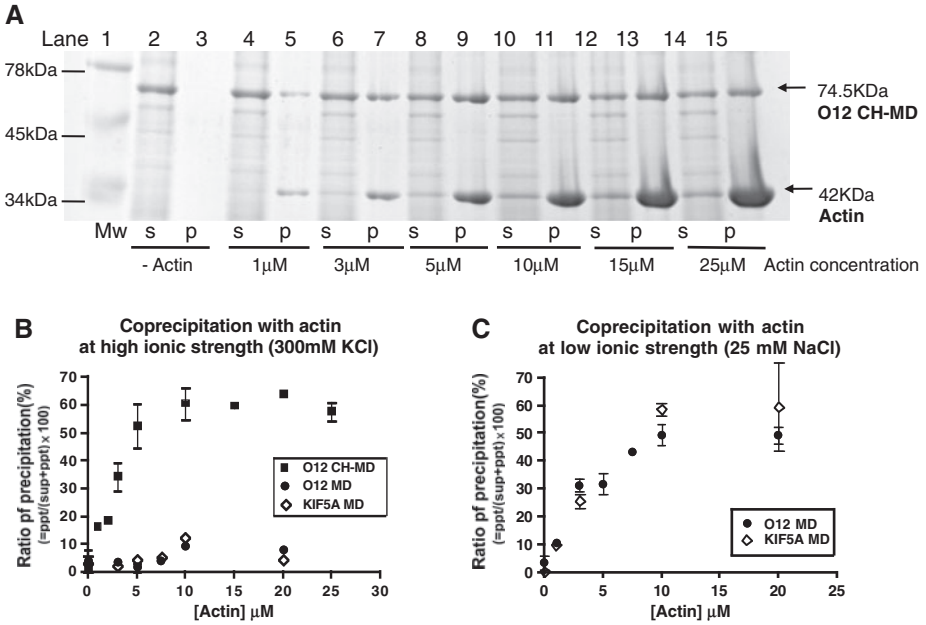

Fig. 7 Actin concentration dependence in a cosedimentation assay of O12CH-MD. (A) Cosedimentation assay of kinesins in the presence or absence of actin. Supernatants (s) and pellets (p) were separated by SDS–PAGE (7.5–20% gels) after centrifugation. Lane 1, molecular weight marker (M; 78 kDa BSA, 45 kDa Ovalbumin, 34 kDa carbonic anhydrase); Lanes 2 and 3, in the absence of actin, Lanes 4–15, in the presence of actin. O12CH-MD bound to actin increased with an increase in actin concentration. (B) and (C) The ratio of precipitation. (B) is high ionic concentration buffer; 300 mM KCl, 3 mM MgCl2, 30 mM pipes pH 6.8, 1 mM DTT. (C) is low ionic concentration buffer; 30 mM NaCl, 3 mM MgCl2, 30 mM pipes pH 6.8, 1 mM DTT. The ratio of precipitation was determined by dividing precipitation (ppt) by the sum of supernatant (sup) and ppt [ppt/(ppt + sup) × 100 = ratio of precipitation (%)]. By using image analyzer software (Image Gauge V4.23), band thickness was quantified. By setting the concentration of the precipitate and that of the supernatant as 1, a graph was drawn to represent the percentage of precipitate of each sample.

constant Ki of 2 μM actin was calculated for the ATPase activity of O12CH-MD in the presence of MT. Interestingly, the ATPase activity of O12MD without the CH domain was also decreased with an increase in actin concentration. However, the effect of actin was weaker than in the case of O12CH-MD, with an estimated Ki of ~20 μM. On the other hand, the MT-dependent ATPase activity of the conventional kinesin was not affected by addition of actin (Fig. 6A).

In the absence of MT, no significant decrease in the ATPase activity of O12CH-MD or O12MD was observed (Fig. 6B). These findings suggested that actin binds to both the CH domain and motor domain to result in inhibition of MT binding or of the MT dependency of ATPase activity.

We also examined the interaction of O12 with actin by co-sedimentation assays. Conventional kinesin KIF5A MD, O12MD and O12CH-MD were incubated with actin and centrifuged to separate the supernatant from the precipitate, which contained O12 bound to actin. The O12 bound to actin was analyzed by SDS–PAGE (Fig. 7). In the absence of actin, all O12CH-MD remained in the supernatant (Fig. 7A, lane 2). In the presence of actin, O12CH-MD bound to actin increased with an increase in actin concentration at high ionic strength (Fig. 7A, lanes 4–15). O12CH-MD bound to actin in the SDS–PAGE (Fig. 7A) was quantified and plotted in Fig. 7B. The binding of O12CH-MD to actin was saturated at 10 μM actin. The estimated Kd from the saturation curve in Fig. 7B was ~3 μM. However, no significant binding of O12MD or conventional kinesin to actin was observed in the high ionic strength buffer (300 mM KCl). On the other hand, O12MD and conventional kinesin bound to actin at low ionic strength as shown in Fig. 7C. The results suggested that the interaction of O12MD with actin is due to electrostatic binding that results in reduction of ATPase activity at low ionic strength. Interestingly, although conventional kinesin bound to actin at low ionic strength, the ATPase activity was not influenced.

Localization of O12 in plant cells

To clarify the physiological roles of O12, the localization of O12 in plant cells was examined. As shown in Fig. 8A, we prepared cDNA encoding the tail of O12 fused with GFP which was inserted into a plasmid for a plant cell expression system. We also tied to prepare full-length O12-GFP. However, we could not succeed to establish the expression of full-length O12-GFP in onion cell at this stage. By using the particle-gun technique, the plasmid was introduced into onion cells. The fluorescence from O12tail-GFP expressed in onion cells was observed as filaments throughout the cell (Fig. 8B-a, c). The filament shape was highly similar to that previously reported for actin filaments (*29*). We also stained the actin with rhodamine-phalloidin in the onion cell in which O12 tail-GFP was expressed (Fig. 8B-e, h). As shown in Fig. 8B-f and -i, the configuration of the actin filaments fluorescently stained by rhodamin-phalloidin was well indentical to that of the filaments labelled by CH-domain-GFP. Therefore, these results suggested that the CH domain of O12 can interact with actin filament in plant cells.

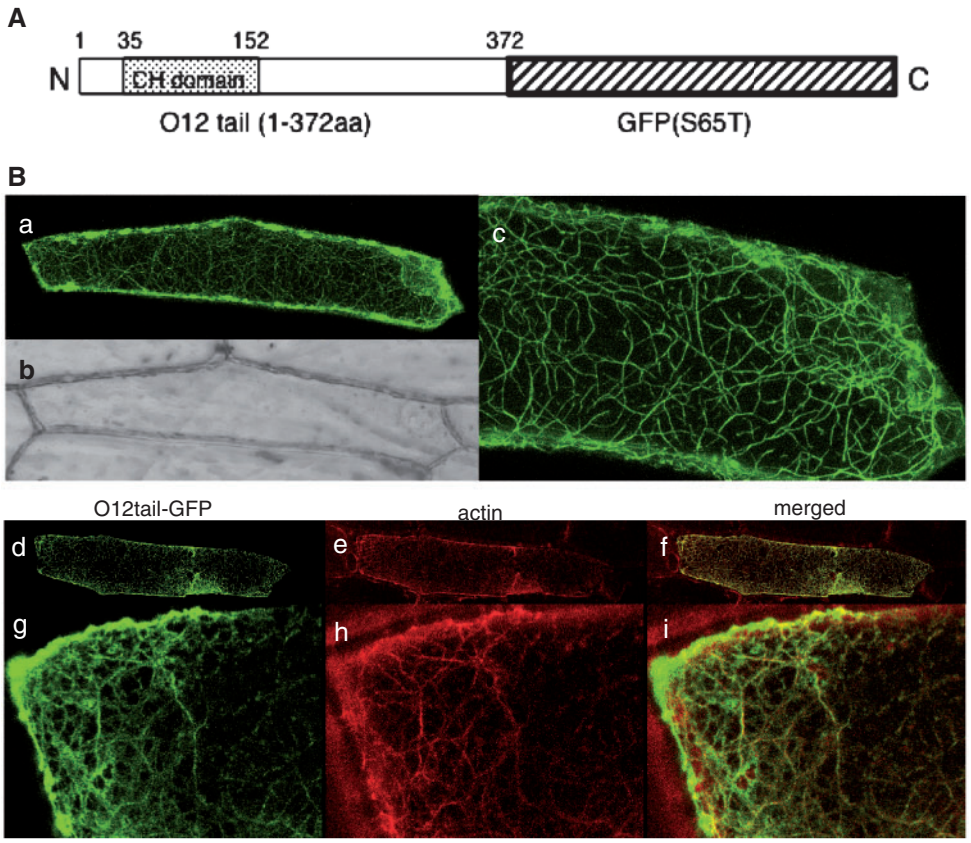

Fig. 8 Intracellular localization of GFP-tagged rice kinesin O12 tail in onion cells. (A) Schematic representation of the structure of the O12 CH domain and coiled-coil region (O12tail, 1–372 amino acids) fused with green fluorescent protein GFP (S65T), which was used for GFP expression in plant cells. (B) GFP-fused O12 tail was observed in onion cells after bombardment. Photomicrographs (a), (c), (d) and (g) are fluorescence images of O12tail-GFP; (c) is a higher magnification image of a portion of the cell shown in (a). Photomicrograph (b) is the light-microscopic view of the cell shown in (a). Photomicrograph (e) and (h) are fluorescence images of rhodamine-phalloidin. Photomicrograph (f) and (i) are fluorescence images merged of O12tail-GFP (d and g) and rhodamine-phalloidin (e and h). The CH domain of O12 localized predominantly to the cytoskeleton.

Discussion

The aim of the present study was to characterize a rice kinesin with unique plant-specific characteristics and to clarify its physiological role. Kinesins are known to be involved in diverse cellular roles in animals, and are also expected to relate to important cellular functions in plants. The study of plant kinesins has lagged behind that of animal kinesins. Recently, studies on plant kinesins derived from species including *A. thaliana*, cotton and tobacco (*Nicotiana tabacum*) have been conducted, in addition to our investigations of rice plant kinesins. Compared to animal kinesins, some plant kinesin have been reported to show unique characteristics (*21*). These unique kinesins may have important plant-specific physiological roles.

In the present study, we focused on the rice-specific kinesin O12. O12 belongs to the kinesin-14 family, which is predominantly comprised of plant kinesins (Figs 1 and 2). The most unique property of O12 is that it contains a CH domain that is believed to interact with actin. The CH domain has been observed specifically in higher plant kinesins and has not been found in any animal kinesin. O12 has been speculated to play a major physiological role in plants that form actin networks.

Stopped-flow experiments revealed that the initial binding of O12 to ATP was unusually slow in the absence of MT compared with that of other kinesins. In contrast, the binding velocity of ATP to O12 was activated by MT at the normal amplification ratio. It is speculated that the ATPase site of O12 may have a closed conformation in the absence of MT, and MT binding induces a conformational change in the ATPase site to increase accessibility to ATP. However, the MT-dependent ATPase activity of O12 was much slower than that of a kinesin derived from animals. Other plant kinesins have also demonstrated relatively lower MT-dependent ATPase activity. This difference may be due to structural differences in MT between plants and animals (*30–32*). Recombinant O12 containing a CH domain and coiled-coil region did not show motility activity on MT derived from porcine brain, which may also be due to conformational differences in MT. In a preliminary experiment, MT crudely prepared from pear and ginkgo pollen accelerated the ATPase activity of the rice plant-specific kinesin K16 more significantly than conventional kinesin.

The unique CH domain of O12 is of interest to us because the domain, observed in microtubule-dependent motor protein kinesins, interacts with

actin, which in turn interacts with myosin, another ATP-driven motor protein. We have confirmed that the CH domain of O12 actually interacts with actin in plant cells, as shown in Fig. 8. Other plant KCHs have also been demonstrated to localize to actin filaments in GhKCH1 and GhKCH2 cotton cells and OsKCH tobacco BY-2 cells (*26*, *28–30*). However, the interaction of the CH domain with actin and the effect of actin on the function of kinesins at the molecular level had not been studied previously.

In this study, we performed biochemical analyses on the effect of actin on the kinesin O12 ATPase activity. As shown in Fig. 6A, actin significantly reduced the MT-dependent ATPase activity of O12CH-MD at a Ki of ~2 μM. In contrast, actin affected the ATPase activity of O12CH-MD slightly in the absence of MT. Therefore, actin binds to the CH domain and hinders MT binding. The significant binding of actin to O12MD-CH was also confirmed by a cosedimentation experiment (Fig. 7). The Kd estimated from the experiments was consistent with the Ki value determined in the ATPase inhibition experiment. Unexpectedly, the MT-dependent ATPase activity of O12MD was also decreased by actin, while O12MD ATPase activity in the absence of MT was not affected by actin (Fig. 6B). Therefore, actin binding to O12MD also hinders interaction with MTs. The ATPase activity of the conventional kinesin MD was not affected at all by actin, which supported the hypothesis that actin binding to the MD is a unique characteristic of kinesin O12. Moreover, this unique property may also be of interest to studies concerning the existence of a common ancestor among the ATP-driven actin- and microtubule-dependent motor proteins originally hypothesized by Kull *et al.* (*43*).

In conclusion, rice plant-specific kinesin O12 containing a CH domain has unique enzymatic properties. The microtubule-dependent ATPase activity of O12 was regulated by actin binding, which may reflect plant-specific physiological roles.

Acknowledgements

We wish to thank Aya Koga-Kitajima and Yuki Hamada (Department of Applied Biological Chemistry, Niigata University) for the excellent assistance in the observation in onion cells using a confocal laser scanning microscope.

Funding

Grant-in-Aid for Scientific Research C (*19570047*) from the Ministry of Education, Culture, Sports, Science and Technology of Japan.

Conflict of interest

None declared.

References

1. Hirokawa, N. and Noda, Y. (2008) Intracellular transport and kinesin superfamily proteins, KIFs: structure, function, and dynamics. *Physiol. Rev.* **88**, 1089–1118
2. Hirokawa, N., Noda, Y., Tanaka, Y., and Niwa, S. (2009) Kinesin superfamily motor proteins and intracellular transport. *Nat. Rev. Mol. Cell Biol.* **10**, 682–696
3. Miki, H., Okada, Y., and Hirokawa, N. (2005) Analysis of the kinesin superfamily: insights into structure and function. *Trends Cell Biol.* **15**, 467–476
4. Vale, R.D. (2003) The molecular motor toolbox for intracellular transport. *Cell* **112**, 467–480
5. Lu, L., Lee, Y.R., Pan, R., Maloof, J.N., and Liu, B. (2005) An internal motor kinesin is associated with the Golgi apparatus and plays a role in trichome morphogenesis in Arabidopsis. *Mol. Biol. Cell* **16**, 811–823
6. Mathur, J. and Chua, N.H. (2000) Microtubule stabilization leads to growth reorientation in Arabidopsis trichomes. *Plant Cell* **12**, 465–477
7. Reddy, A.S. and Day, I.S. (2001) Kinesins in the Arabidopsis genome: a comparative analysis among eukaryotes. *BMC Genomics* **2**, 2
8. Tamura, K., Nakatani, K., Mitsui, H., Ohashi, Y., and Takahashi, H. (1999) Characterization of katD, a kinesin-like protein gene specifically expressed in floral tissues of Arabidopsis thaliana. *Gene* **230**, 23–32
9. Dymek, E.E., Goduti, D., Kramer, T., and Smith, E.F. (2006) A kinesin-like calmodulin-binding protein in Chlamydomonas: evidence for a role in cell division and flagellar functions. *J. Cell. Sci.* **119**, 3107–3116
10. Abdel-Ghany, S.E., Day, I.S., Simmons, M.P., Kugrens, P., and Reddy, A.S. (2005) Origin and evolution of Kinesin-like calmodulin-binding protein. *Plant Physiol.* **138**, 1711–1722
11. Reddy, V.S. and Reddy, A.S. (1999) A plant calmodulin-binding motor is part kinesin and part myosin. *Bioinformatics* **15**, 1055–1057
12. Jiang, S., Li, M., Xu, T., Ren, D., and Liu, G. (2007) Two kinesins from Arabidopsis, KatB and KatC, have a second microtubule-binding site in the tail domain. *J. Biochem. Mol. Biol.* **40**, 44–52
13. Mitsui, H., Nakatani, K., Yamaguchi-Shinozaki, K., Shinozaki, K., Nishikawa, K., and Takahashi, H. (1994) Sequencing and characterization of the kinesin-related genes katB and katC of Arabidopsis thaliana. *Plant Mol. Biol.* **25**, 865–876
14. Preuss, M.L., Delmer, D.P., and Liu, B. (2003) The cotton kinesin-like calmodulin-binding protein associates with cortical microtubules in cotton fibers. *Plant Physiol.* **132**, 154–160
15. Sazuka, T., Aichi, I., Kawai, T., Matsuo, N., Kitano, H., and Matsuoka, M. (2005) The rice mutant dwarf bamboo shoot 1: a leaky mutant of the NACK-type kinesin-like gene can initiate organ primordia but not organ development. *Plant Cell Physiol.* **46**, 1934–1943
16. Dagenbach, E.M. and Endow, S.A. (2004) A new kinesin tree. *J. Cell. Sci.* **117**, 3–7
17. Hamada, T. (2007) Microtubule-associated proteins in higher plants. *J. Plant Res.* **120**, 79–98
18. Asada, T., Kuriyama, R., and Shibaoka, H. (1997) TKRP125, a kinesin-related protein involved in the centrosome-independent organization of the cytokinetic apparatus in tobacco BY-2 cells. *J. Cell. Sci.* **110**, 179–189
19. Ambrose, J.C. and Cyr, R. (2008) Mitotic spindle organization by the preprophase band. *Mol. Plant* **1**, 950–960
20. Richardson, D.N., Simmons, M.P., and Reddy, A.S. (2006) Comprehensive comparative analysis of kinesins in photosynthetic eukaryotes. *BMC Genomics* **7**, 18
21. Umeki, N., Mitsui, T., Umezu, N., Kondo, K., and Maruta, S. (2006) Preparation and characterization of a novel rice plant-specific kinesin. *J. Biochem.* **139**, 645–654
22. Umeki, N., Mitsui, T., Kondo, K., and Maruta, S. (2006) Conformational change of the loop L5 in rice kinesin

motor domain induced by nucleotide binding. *J. Biochem.* **139**, 857–864
23. Tanaka, K, Umeki, N, Toshiaki, M, Fujimoto, Z, and Maruta, S. (2010) Crystallographic analysis reveals a unique conformation of the ADP-bound novel rice kinesin K16. *Biochem Biophys Res Commun*. **401**, 251–256
24. Gimona, M., Djinovic-Carugo, K., Kranewitter, W.J., and Winder, S.J. (2002) Functional plasticity of CH domains. *FEBS Lett*. **513**, 98–106
25. Friedberg, F. (2010) Single and multiple CH (calponin homology) domain containing multidomain proteins in Arabidopsis and Saccharomyces: an inventory. *Mol. Biol. Rep*., in press
26. Preuss, M.L., Kovar, D.R., Lee, Y.R., Staiger, C.J., Delmer, D.P., and Liu, B. (2004) A plant-specific kinesin binds to actin microfilaments and interacts with cortical microtubules in cotton fibers. *Plant Physiol.* **136**, 3945–3955
27. Xu, T., Sun, X., Jiang, S., Ren, D., and Liu, G. (2007) Cotton GhKCH2, a plant-specific kinesin, is low-affinitive and nucleotide-independent as binding to microtubule. *J. Biochem. Mol. Biol*. **40**, 723–730
28. Xu, T., Qu, Z., Yang, X., Qin, X., Xiong, J., Wang, Y., Ren, D., and Liu, G. (2009) A cotton kinesin GhKCH2 interacts with both microtubules and microfilaments. *Biochem. J*. **421**, 171–180
29. Frey, N., Klotz, J., and Nick, P. (2009) Dynamic bridges: a calponin-domain kinesin from rice links actin filaments and microtubules in both cycling and non-cycling cells. *Plant Cell Physiol*. **50**, 1493–1506
30. Petrásek, J. and Schwarzerová, K. (2009) Actin and microtubule cytoskeleton interactions. *Curr. Opin. Plant Biol*. **12**, 728–734
31. Koo, B.S., Kalme, S., Yeo, S.H., Lee, S.J., and Yoon, M.Y. (2009) Molecular cloning and biochemical characterization of alpha- and beta-tubulin from potato plants (Solanum tuberosum L.). *Plant Physiol. Biochem*. **47**, 761–768
32. Mineyuki, Y. (2007) Plant microtubule studies: past and present. *J. Plant Res*. **120**, 45–51
33. Hackney, D.D. (1988) Kinesin ATPase: rate-limiting ADP release. *Proc. Natl Acad. Sci. USA* **85**, 6314–6318
34. Mommaerts, W.F. (1951) Reversible polymerization and ultracentrifugal purification of actin. *J. Biol. Chem*. **188**, 559–565
35. Shimizu, T., Sablin, E., Vale, R.D., Fletterick, R., Pechatnikova, E., and Taylor, E.W. (1995) Expression, purification, ATPase properties, and microtubule-binding properties of the ncd motor domain. *Biochemistry* **34**, 13259–13266
36. Youngburg, G.E. and Youngburg, M.V. (1930) A system of blood phosphorus analysis. *J. Lab. Clin. Med.* **16**, 158–166
37. Maruta, S., Mizukura, Y., and Chaen, S. (2002) Interaction of a new fluorescent ATP analogue with skeletal muscle myosin subfragment-1. *J. Biochem*. **131**, 905–911
38. Kitajima, A., Asatsuma, S., Okada, H., Hamada, Y., Kaneko, K., Nanjo, Y., Kawagoe, Y., Toyooka, K., Matsuoka, K., Takeuchi, M., Nakano, A., and Mitsui, T. (2009) The rice alpha-amylase glycoprotein is targeted from the Golgi apparatus through the secretory pathway to the plastids. *Plant Cell* **21**, 2844–2858
39. Ma, Y.Z. and Taylor, E.W. (1997) Kinetic mechanism of a monomeric kinesin construct. *J. Biol. Chem*. **272**, 717–723
40. Cochran, J.C., Krzysiak, T.C., and Gilbert, S.P. (2006) Pathway of ATP hydrolysis by monomeric kinesin Eg5. *Biochemistry* **45**, 12334–12344
41. Cochran, J.C., Sontag, C.A., Maliga, Z., Kapoor, T.M., Correia, J.J., and Gilbert, S.P. (2004) Mechanistic analysis of the mitotic kinesin Eg5. *J. Biol. Chem*. **279**, 38861–38870
42. Mackey, A.T. and Gilbert, S.P. (2000) Moving a microtubule may require two heads: a kinetic investigation of monomeric Ncd. *Biochemistry* **39**, 1346–1355
43. Kull, F.J., Vale, R.D., and Fletterick, R.J. (1998) The case for a common ancestor: kinesin and myosin motor proteins and G proteins. *J. Muscle Res. Cell. Motil*. **19**, 877–886